Chemical Science

ROYAL SOCIETY OF CHEMISTRY

EDGE ARTICLE

View Article Online
View Journal | View Issue

Cite this: *Chem. Sci.*, 2023, **14**, 14211

All publication charges for this article have been paid for by the Royal Society of Chemistry

Received 1st September 2023
Accepted 20th November 2023

DOI: 10.1039/d3sc04613c

rsc.li/chemical-science

Solution-state mechanochromic luminescence of Pt(II)-complexes displayed within micellar aromatic capsules†

Yoshihisa Hashimoto, Yuri Katagiri, Yuya Tanaka * and Michito Yoshizawa *

Mechanochromic luminescence (MCL) is an intrinsic phenomenon *in the solid state* and thus has been hardly observed in solution so far. Here we report that arylethynyl Pt(II)-complexes with an NCN-pincer ligand are efficiently encapsulated by micellar aromatic capsules in water, through a simple grinding protocol with bent amphiphiles. When a bent pentamethylbenzene-based amphiphile is employed as an optimized capsule component, the resultant host–guest composite, with an average diameter of ~4 nm, is obtained in water at room temperature. Notably, the nanocomposite displays strong red emission (Φ = 33%, λ_{max} = 700 nm) derived from MCL *via* intermolecular Pt(II)···Pt(II) interactions even under aerobic aqueous conditions, in sharp contrast to the free Pt(II)-complex with weak green emission (Φ = 4%, λ_{max} = 500 nm) in CH_2Cl_2. Moreover, enhancement of the solution-state MCL (up to Φ = 48%) can be achieved by coencapsulation of the Pt(II)-complexes with carbazole derivatives by the capsule in water. This study provides the first example of "solution-state" mechanochromic luminescence, capable of facilely tuning its intensity and wavelength, among the intensive studies of various solid-state MCL reported previously.

Introduction

Organic molecules and metal-complexes providing mechanochromic luminescent (MCL) properties have received increasing attention over the last decade, because of their potential applications for sensors, memory devices, and security technologies.[1] A wide variety of MCL compounds were rationally and accidentally synthesized so far.[1,2] Among them, unlike organic MCL molecules, mechanochromic Pt(II),[3] Au(I),[1c,2a] and Cu(I)-complexes[2c] display medium to strong luminescence with long wavelengths (*i.e.*, visible and near-IR regions), *via* the *in situ* formation of intermolecular metal···metal interactions between the metal-complexes, by mechanochemical stimuli such as manual grinding or mechanical ball milling (Fig. 1a). However, such appealing MCL behavior can be observed only in the solid state,[1c,3,4] owing to the instability of the metal···metal interactions, which fully dissociate *in solution*. Even in ground solids, the MCL states easily return back to the thermodynamically stable initial state by heating or solvent vapor exposure. To the best of our knowledge, successful generation of the MCL states has never been demonstrated to date in not only organic solvents but also environmentally benign water.[5] We envisioned that solution-state MCL features could be observed by the supramolecular encapsulation of MCL nanoparticles from MCL solids (Fig. 1b, top). We herein report the encapsulation of MCL-active Pt(II)-complexes as nanoparticles by micellar aromatic capsules in water. When NCN-pincer Pt(II)-complexes **1a–c** are encapsulated by pentamethylbenzene-based micellar capsule $(\mathbf{PBA})_n$ (Fig. 1c) *via* a grinding method, the

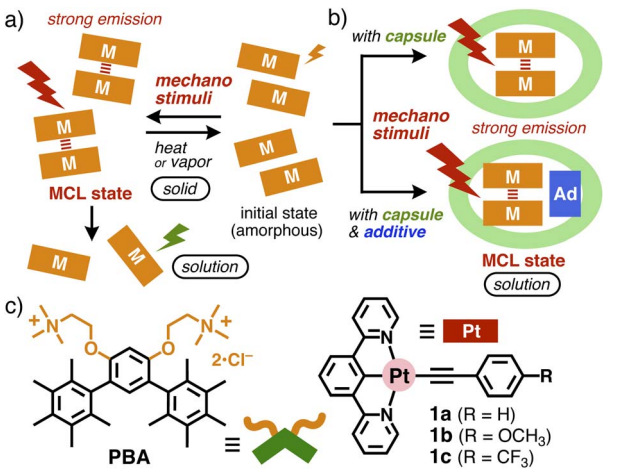

Fig. 1 Mechanochromic luminescent (MCL) behavior of metal-complexes (a) in the solid state and *in solution*, and (b) within a molecular capsule in solution, without/with additives (this work). (c) Bent aromatic amphiphile **PBA** and NCN-pincer Pt(II)-complexes **1a–c**.

Laboratory for Chemistry and Life Science, Institute of Innovative Research, Tokyo Institute of Technology, 4259 Nagatsuta, Midori-ku, Yokohama 226-8503, Japan. E-mail: yoshizawa.m.ac@m.titech.ac.jp; ytanaka@res.titech.ac.jp

† Electronic supplementary information (ESI) available. CCDC 2269104. For ESI and crystallographic data in CIF or other electronic format see DOI: https://doi.org/10.1039/d3sc04613c

resultant host–guest composites show strong red luminescence, on the basis of intermolecular metal-metal-to-ligand charge transfer (MMLCT) interactions, in high quantum yields ($\Phi = 33\%$ for **1a**) in aqueous solution. In addition, the solution-state MCL can be further enhanced by 1.5-fold upon coencapsulation of **1a** with carbazole derivatives as additives by the capsule (Fig. 1b, bottom).

Arylethynyl Pt(II)-complexes **1a–c** are phosphorescent compounds with an NCN-pincer ligand (Fig. 1c, right), featuring a tridentate ligand with a carbon-based strong σ donor, which enhances their emission properties.[6] The square planar geometry allows them to stack to each other without metal···metal interactions in the solid state.[6] Under aerobic conditions, the solid can emit moderate luminescence in a stacked fashion, whereas the emission abilities of the Pt(II)-complexes largely decrease in solution (*e.g.*, CH_2Cl_2 and THF), due to emission quenching by oxygen, which prevents their sensor application under practical conditions. There have been intensive studies on the formation of infinite columnar stacks of arylethynyl Pt(II)-complexes, providing large functional groups for intermolecular interactions.[7] Kinetic control of the columnar/particle assemblies of amphiphilic Pt(II)-complexes has been developed.[8] However, the previous infinite stacks cannot display MCL properties and the encapsulation of MCL-active metal-complexes has not been accomplished even by molecular hosts.[7,9] Bent aromatic amphiphile **PBA**, synthesized in this work as an optimized water-solubilizing reagent for **1a–c** in MCL states, is composed of two pentamethylbenzene panels linked with a *m*-phenylene spacer with two trimethylammonium groups (Fig. 1b).[10,11] The new cationic amphiphiles form micellar capsule $(\mathbf{PBA})_n$ with a spherical aromatic shell in water through the hydrophobic effect and multiple CH–π interactions. As compared with previously reported derivatives with polyaromatic panels (*e.g.*, anthracene, acridine, and phenothiazine),[12,13] **PBA** is transparent in the visible range ($\lambda > 300$ nm), which is beneficial for photo-active guest molecules. Notably, an efficient coencapsulation with additives (Fig. 1b, bottom), succeeded herein for the first time in micellar capsules, further enhances solution-state MCL from the Pt(II)-complexes, due to reduction in the aggregation of MCL-active species within the capsule.

Results and discussion

Efficient uptake of arylethynyl Pt(II)-complexes

As the first attempt, the water solubilizing ability of amphiphilic compounds toward highly hydrophobic Pt(II)-complex **1a** with a phenylethynyl group was investigated under various conditions. The study revealed a higher efficiency with bent aromatic amphiphiles (*i.e.*, **PBA**, **PBS**,[11] and **AA**) over aliphatic amphiphiles (*i.e.*, **ADA**,[14] **SDS**, and **DTAC**).[15] As the optimized procedure, a mixture of solids **PBA** and **1a** (2.0 μmol each) was manually ground for ~2 min using an agate mortar and pestle and the resultant solid was dissolved in H_2O (1.0 mL) at room temperature.[15] The centrifugation and filtration of the suspended mixture gave rise to a clear yellow solution including host–guest composite $(\mathbf{PBA})_n\cdot(\mathbf{1a})_m$ (Fig. 2a, right). The UV-visible spectrum showed a new, broad absorption band at $\lambda_{max} = 400$ nm, derived from encapsulated $(\mathbf{1a})_m$ in capsule $(\mathbf{PBA})_n$ (Fig. 2b).[16] The absorption is slightly shifted by +7 nm, relative to free **1a** in CH_2Cl_2, upon encapsulation, owing to host–guest interactions (*e.g.*, the hydrophobic effect and CH–π interactions). The relative solubilization efficiency was estimated on the basis of the band intensity at 400 nm for $(\mathbf{PBA})_n\cdot(\mathbf{1a})_m$ and various host–guest composites, obtained by the combination of **1a** with **PBS**, **AA**, **ADA**, **SDS**, or **DTAC** (Fig. S24†).[15] As compared with **PBA**, the efficiency increased with **PBS** and **AA** (≥1.2-fold) yet decreased with **ADA**, **SDS**, and **DTAC** (<0.3-fold) under the same conditions (Fig. 2c), suggesting the necessity of the bent aromatic frameworks. The concentration of **1a** solubilized in water was calculated to be 0.1 mM by ^{1}H NMR analysis in CD_3OD after the lyophilization of $(\mathbf{PBA})_n\cdot(\mathbf{1a})_m$ (Fig. S21b†).

It is important to note that, besides the intense band at 400 nm, a new shoulder band was observed at 460–590 nm in the UV-visible spectrum of $(\mathbf{PBA})_n\cdot(\mathbf{1a})_m$ (Fig. 2b, inset). The absorption band is assignable to the intermolecular Pt(II)···Pt(II) interactions within $(\mathbf{1a})_m$, arising from MMLCT interactions, on the basis of previous literature.[17] Similar bands were found in the UV-visible spectra of $(\mathbf{PBS})_n\cdot(\mathbf{1a})_m$, $(\mathbf{AA})_n\cdot(\mathbf{1a})_m$, and $(\mathbf{ADA})_n\cdot(\mathbf{1a})_m$ (Fig. S23†).[15]

MCL properties of host–guest composites in water

Among the host–guest composites in hand, $(\mathbf{PBA})_n\cdot(\mathbf{1a})_m$ displayed the strongest red MCL in water without degassing. Under

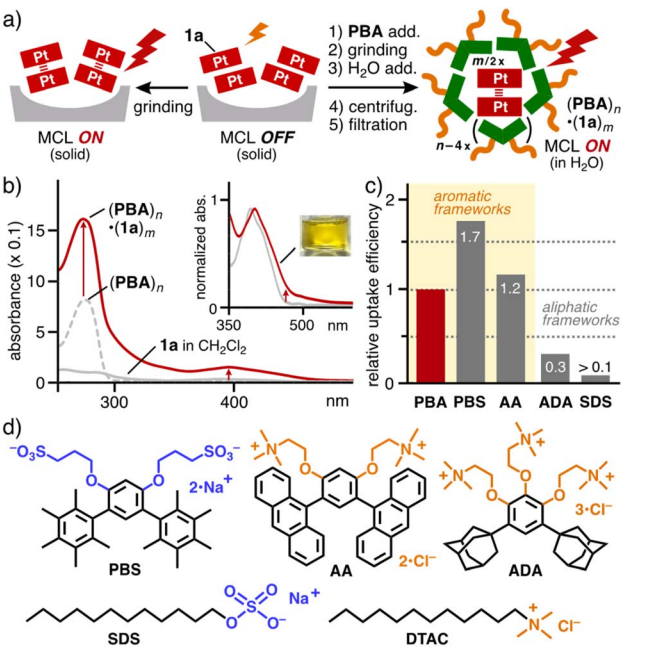

Fig. 2 (a) MCL properties of Pt(II)-complex **1a** with/without **PBA** and the formation of $(\mathbf{PBA})_n\cdot(\mathbf{1a})_m$ in water. (b) UV-visible spectra (H_2O, r.t., 2.0 mM based on **PBA**) of $(\mathbf{PBA})_n\cdot(\mathbf{1a})_m$, $(\mathbf{PBA})_n$, **1a**, and their expanded spectra (inset). (c) Uptake efficiency of host–guest composites obtained from various amphiphiles and **1a**. (d) Bent and linear amphiphiles studied herein.

aerobic conditions, a CH_2Cl_2 solution of **1a** (0.02 mM) showed weak emission bands at 500 nm (green color, $\Phi = 4\%$, $\tau = 0.19$ μs), derived from its monomeric state, upon irradiation at 450 nm (Fig. 3a and c). In sharp contrast, the resultant aqueous solution of $(\mathbf{PBA})_n\cdot(\mathbf{1a})_m$ exhibited a prominent emission band at $\lambda_{max} = 700$ nm with a quantum yield of 33%.[18] The emission lifetime was estimated to be 0.61 μs (Fig. 3c), which is assignable to a stacked Pt(II)-complex dimer with Pt(II)···Pt(II) interactions.

Solid **1a** itself showed broadened emission bands at $\lambda_{max} =$ 600 nm (yellow color, $\Phi = 15\%$), assignable to its typical π-stacked dimer,[6] whereas the band was largely red-shifted to be identical to that of $(\mathbf{PBA})_n\cdot(\mathbf{1a})_m$, upon manual grinding for ~2 min (Fig. 3a).[18] The emission quantum yield and lifetime of ground solid **1a** ($\Phi = 33\%$ and $\tau = 0.60$ μs; Fig. 3c) remained fully intact even after uptake by the capsule. As the control experiment, host–guest composite $(\mathbf{PBA})_n\cdot(\mathbf{1a})_m$, prepared by vigorous stirring a mixture of **PBA** and solid **1a** in water (without grinding), showed weak green emission ($\lambda = 470$–590 nm), merely derived from monomeric **1a** within the capsule (Fig. S44a†).[15,19] Accordingly, MCL-state $(\mathbf{1a})_m$ was successfully encapsulated and solubilized by capsule $(\mathbf{PBA})_n$ through the simple grinding protocol, without the dissociation of the Pt(II)···Pt(II) interactions and usual aggregation-caused emission quenching.

Similar MCL bands yet different intensities were found in the emission spectra of the other host–guest composites under the same conditions (Fig. S26 and S27†). The quantum yields of $(\mathbf{ADA})_n\cdot(\mathbf{1a})_m$ and (**PBS** or **AA**)$_n\cdot(\mathbf{1a})_m$ were slightly lower ($\Phi =$ 28%) and much lower ($\Phi =$ 8–9%) than that of $(\mathbf{PBA})_n\cdot(\mathbf{1a})_m$, respectively (Fig. 3b). These results indicate that the emissivity of the resultant host–guest composites is largely affected by both of the hydrophobic and hydrophilic groups on the bent amphiphiles. Adamantane-based CH–π interactions mostly retain the MCL properties of $(\mathbf{1a})_m$ within $(\mathbf{ADA})_n$, whereas anthracene-based π–π interactions largely prevent the MCL within $(\mathbf{AA})_n$, owing to the π-electron based host–guest interactions. The unexpected, low quantum yield of $(\mathbf{1a})_m$ within $(\mathbf{PBS})_n$, bearing anionic sulfonate groups, suggests the presence of an excited-state deactivation pathway through the hydrophilic groups on the basis of the emission lifetime analysis ($\tau =$ 0.29 μs; Fig. S28†).[15] Linear amphiphile-based host–guest composites (**SDS** or **DTAC**)$_n\cdot(\mathbf{1a})_m$ exhibited low quantum yields ($\Phi = 7$ and <1%, respectively).

The host–guest structure of $(\mathbf{PBA})_n\cdot(\mathbf{1a})_m$ was estimated by the combination of DLS, UV-visible, and luminescence data and molecular modeling studies. The DLS analysis indicated the average core diameter of $(\mathbf{PBA})_n\cdot(\mathbf{1a})_m$ being 3.9 nm, which is expanded by 2.5 nm as compared with that of $(\mathbf{PBA})_n$ (1.4 nm), due to the encapsulation of hydrophobic assemblies $(\mathbf{1a})_m$ (Fig. 4a). Multiple inclusion of stacked dimer $(\mathbf{1a})_2$, as a major subunit, in the spherical shell of $(\mathbf{PBA})_n$ was supported by the observed absorption and emission bands (*i.e.*, ~480 and ~700 nm, respectively; Fig. 2b and 3a). In addition, the X-ray crystal structure of **1c** revealed the formation of a head-to-head stacking dimer with a Pt(II)···Pt(II) distance of 3.3 Å and a twist angle of ~44.4° (Fig. 4c and S18†). On the basis of these findings, molecular modeling studies suggested that the product structure is composed of $(\mathbf{PBA})_{30}\cdot(\mathbf{1a})_{16}$, with an outer diameter of 4.5 nm and a core diameter of 3.9 nm, on an average (Fig. 4b). In the optimized structure, encapsulated $(\mathbf{1a})_{16}$ adopts a roughly spherical structure, including stacked dimers $(\mathbf{1a})_2$ with ~3.3 Å Pt(II)···Pt(II) distances. The presence of multiple CH–π interactions is also suggested between the host and guest hydrophobic frameworks.

Solution-state MCLs could be also observed for other Pt(II)-complexes **1b** and **1c**, with an electron-donating methoxy group and electron-withdrawing trifluoromethyl group, respectively (Fig. 1c), through the grinding protocol with **PBA**.[15] On the basis of the absorption spectra of the resultant host–guest composites, the uptake efficiency of the Pt(II)-complexes and the band intensity (at ~570 nm) derived from the Pt(II)···Pt(II) interactions were comparable to those of $(\mathbf{PBA})_n\cdot(\mathbf{1a})_m$ (Fig. S29†). The broadened MCL bands of $(\mathbf{PBA})_n\cdot(\mathbf{1b})_m$ and $(\mathbf{PBA})_n\cdot(\mathbf{1c})_m$ were found at $\lambda_{max} = 697$ and 690 nm, respectively (Fig. 5a), upon irradiation at 450 nm. Again, the solution-state quantum yields of $(\mathbf{PBA})_n\cdot(\mathbf{1b})_m$ ($\Phi = 34\%$) and $(\mathbf{PBA})_n\cdot(\mathbf{1c})_m$ ($\Phi = 14\%$) were

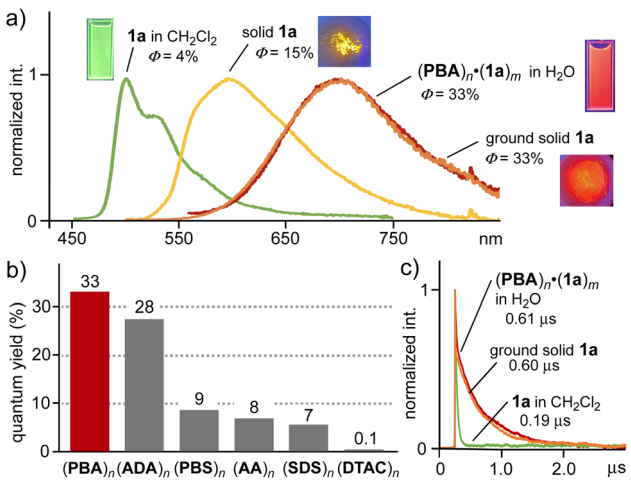

Fig. 3 (a) Emission spectra and their quantum yields (r.t., $\lambda_{ex} = 450$ nm) of **1a** under various conditions and $(\mathbf{PBA})_n\cdot(\mathbf{1a})_m$ in H_2O. (b) Quantum yields of (H_2O, $\lambda_{ex} = 450$ nm) of host–guest composites including **1a** using various amphiphiles. (c) Emission lifetimes (r.t., $\lambda_{ex} = 280$ nm, $\lambda_{det} =$ 500 or 700 nm) of $(\mathbf{PBA})_n\cdot(\mathbf{1a})_m$ in H_2O, **1a** in CH_2Cl_2, and ground solid **1a**.

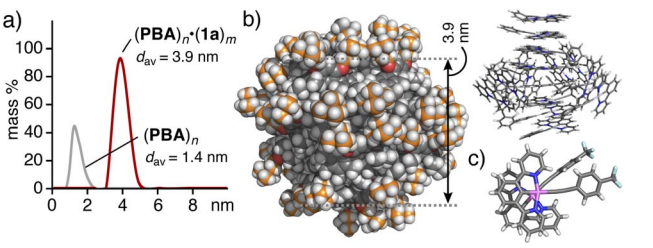

Fig. 4 (a) DLS charts (H_2O, r.t., 1.0/2.0 mM based on PBA) of $(\mathbf{PBA})_n$ and $(\mathbf{PBA})_n\cdot(\mathbf{1a})_m$ (prepared by the grinding method). (b) Optimized structure of $(\mathbf{PBA})_{30}\cdot(\mathbf{1a})_{16}$ (left) and its encapsulated guests (right). (c) Crystal structure of a **1c** dimer.

comparable to those of ground solids **1b** and **1c** (Fig. 5b and S31a†), indicating the excellent uptake ability of $(\mathbf{PBA})_n$, without emission quenching. The CIE diagram of the host–guest composites quantified the total emission colors. While ground solids **1a–c** exhibited a nearly identical color (Fig. 5c), the color was tunable upon encapsulation by the capsule (Fig. 5d).

Coencapusulation-induced enhanced MCL

Successful enhancement (up to 1.5-fold) of the solution-state MCL was finally accomplished within capsule $(\mathbf{PBA})_n$ through a coencapsulation approach. Biscarbazole derivative **BC** was employed herein as an additive with sterically demanding aromatic frameworks.[20] The same grinding protocol, described above, using a 1 : 1 : 1 mixture of **PBA**, **1a**, and **BC** (2.0 μmol each), led to the selective formation of ternary host–guest composite $(\mathbf{PBA})_n\cdot(\mathbf{1a})_m\cdot(\mathbf{BC})_p$ in water as a clear yellow solution, after removal of suspended excess guests (Fig. 6a).[21] The UV-visible spectrum of the ternary composite showed absorption bands, derived from both $(\mathbf{1a})_2$ with MMLCT interactions and **BC**, in the range of 460–590 and 310–370 nm, respectively (Fig. 6b). The DLS and AFM analyses indicated the formation of large spherical particles with average sizes of 13–14 nm (Fig. 6d–f, S39 and S40).[15] The average ratio of **PBA** and encapsulated guests **1a** and **BC** was estimated to be 10 : 2 : 3 ($=n:m:p$) by the ^{1}H NMR analysis of the lyophilized product in DMSO-d_6 (Fig. S34b†).

Remarkably, the aqueous solution of $(\mathbf{PBA})_n\cdot(\mathbf{1a})_m\cdot(\mathbf{BC})_p$ displayed an intense emission band at λ_{max} = 687 nm and its emission quantum yield was found to be 48% (λ_{ex} = 450 nm, Fig. 6c). The observed emission enhancement (1.5 times) upon coencapsulation is most probably caused by reduction of the tight aggregation of dimers $(\mathbf{1a})_2$ with an MCL-active state in the cavity of capsule $(\mathbf{PBA})_n$.[22] The reduced aggregation and quenching process were supported by the blue-shift of the MCL band ($\Delta\lambda = -13$ nm) and the elongation of the MCL lifetime ($\Delta\tau$ = +10 ns, Fig. 6g), respectively, relative to those of $(\mathbf{PBA})_n\cdot(\mathbf{1a})_m$. Other additives such as carbazole (**Cz**), *N*-phenylcarbazole, biphenyl, and coronene showed no to slight emission enhancement (Φ = 10–37%) even upon coencapsulation with **1a** by the capsule under the same conditions (Fig. 6c and S36†).[15] The MCL of solid **1a** was enhanced by 1.4 times (Φ = 45%) upon co-grinding with **BC** (1.0 equiv.) for ~2 min (Fig. S41a†).

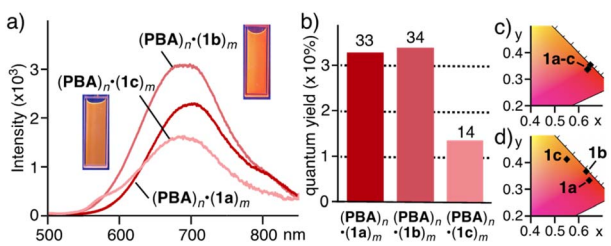

Fig. 5 (a) Emission spectra and photographs (H_2O, r.t., 2.0 mM based on **PBA**, λ_{ex} = 450 nm) of $(\mathbf{PBA})_n\cdot(\mathbf{1a–c})_m$ (prepared by the grinding method) and (b) their quantum yields. CIE diagrams (r.t., λ_{ex} = 450 nm) of (c) ground solids **1a–c** and (d) **1a–c** within $(\mathbf{PBA})_n$ in water.

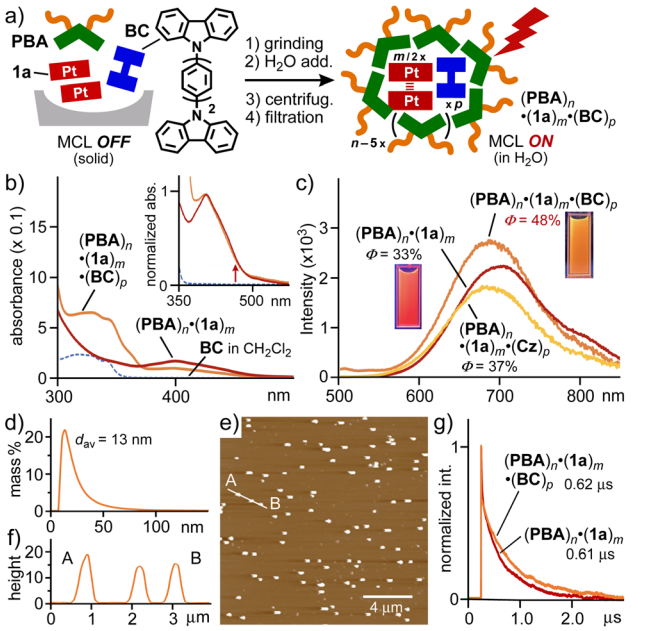

Fig. 6 (a) MCL enhancement of **1a** upon coencapsulation with **BC** by $(\mathbf{PBA})_n$ in water. (b) UV-visible spectra (H_2O, r.t., 2.0 mM based on **PBA**) of $(\mathbf{PBA})_n\cdot(\mathbf{1a})_m\cdot(\mathbf{BC})_p$, $(\mathbf{PBA})_n\cdot(\mathbf{1a})_m$, **BC** in CH_2Cl_2, and their expanded spectra (inset). (c) Emission spectra and their quantum yields (r.t., λ_{ex} = 450 nm) of $(\mathbf{PBA})_n\cdot(\mathbf{1a})_m\cdot(\mathbf{BC}$ or $\mathbf{Cz})_p$ and $(\mathbf{PBA})_n\cdot(\mathbf{1a})_m$ in H_2O. (d) DLS chart (H_2O, r.t., 0.1 mM based on **PBA**) of $(\mathbf{PBA})_n\cdot(\mathbf{1a})_m\cdot(\mathbf{BC})_p$. (e) AFM image (dry, r.t., mica) of $(\mathbf{PBA})_n\cdot(\mathbf{1a})_m\cdot(\mathbf{BC})_p$ and (f) the selected height (nm) profile. (g) Emission lifetimes (H_2O, r.t., λ_{ex} = 280 nm, λ_{det} = 700 nm) of $(\mathbf{PBA})_n\cdot(\mathbf{1a})_m$ and $(\mathbf{PBA})_n\cdot(\mathbf{1a})_m\cdot(\mathbf{BC})_p$.

Conclusions

We have succeeded in the generation of solution-state mechanochromic luminescence (MCL) from Pt(II)-complexes upon encapsulation by aromatic capsules in water. The MCLs, derived from both inorganic and organic compounds, have so far been only observed in the solid state, whereas manual grinding is a facile external stimulus. When NCN-pincer Pt(II)-complexes were encapsulated by the capsule, composed of bent aromatic amphiphiles, *via* a simple grinding method, the resultant host–guest composite exhibited strong red MCL (Φ = 33%), derived from intermolecular Pt(II)···Pt(II) interactions, under aerobic aqueous conditions. Notably, the emission quantum yield and emission color of the Pt(II)-complex were significantly enhanced (*i.e.*, up to 8-fold) and largely altered (*i.e.*, from green to red, $\Delta\lambda$ = up to 200 nm) upon the encapsulation, as compared with those in solution (CH_2Cl_2). Such large changes cannot be accomplished even with fluorescent aromatic compounds, owing to strong aggregation-caused emission quenching. Thanks to the flexible capsule framework, unlike covalent and coordination hosts with rigid frameworks, a ternary host–guest composite was efficiently and selectively obtained through the same grinding protocol using a biscarbazole-based additive. The quantum yield was surprisingly increased to be ~50%, due to the coencapsulation effect. It is worthy of note that this study provides the first example of

"solution-state" MCL, capable of facilely tuning its emission intensity and wavelength, among the intensive studies of various solid-state MCL reported previously.[1c,2–4] We hope that the present method could be applied to not only other Pt(II)-complexes but also inorganic/organic MCL compounds, for the creation of new functional MCL-based supramolecular nano-tools useable in solution. Particularly, from the viewpoints of the high accessibility, water-solubility, and air-insensitivity of this system, biological applications as novel luminescent sensors featuring strong emissivity in the near-infrared region will be more promising, *via* attaching exterior functional groups (*e.g.*, saccharides and peptides)[23] on the aromatic capsules.

Data availability

The experimental procedures and analytical data are available in the ESI†.

Author contributions

Y. H., Y. K., Y. T., and M. Y. designed the work, carried out research, analyzed data, and wrote the paper. M. Y. is the principal investigator. All authors discussed the results and commented on the manuscript.

Conflicts of interest

There are no conflicts to declare.

Acknowledgements

This work was supported by JSPS KAKENHI (Grant No. JP21K18951/JP22H00348) and The Mitsubishi Foundation (Research Grants in the Natural Sciences), Shorai Foundation for Science and Technology, and Research Foundation for the Electrotechnology of Chubu. The theoretical calculations were performed by using computers in the Research Center for Computational Science, Okazaki, Japan (22-IMS-C071, 23-IMS-C063).

Notes and references

1 Representative reviews on organic and inorganic MCL:(*a*) A. P. Haehnel, Y. Sagara, Y. C. Simon and C. Weder, *Top. Curr. Chem.*, 2015, **369**, 345–376; (*b*) Y. Sagara, S. Yamane, M. Mitani, C. Weder and T. Kato, *Adv. Mater.*, 2016, **28**, 1073–1095; (*c*) T. Seki and H. Ito, *Chem.–Eur. J.*, 2016, **22**, 4322–4329.

2 Pioneering MCL works:(*a*) H. Ito, T. Saito, N. Oshima, N. Kitamura, S. Ishizaka, Y. Hinatsu, M. Wakeshima, M. Kato, K. Tsuge and M. Sawamura, *J. Am. Chem. Soc.*, 2008, **130**, 10044–10045; (*b*) G. Zhang, J. Lu, M. Sabat and C. L. Fraser, *J. Am. Chem. Soc.*, 2010, **132**, 2160–2162; (*c*) S. Perruchas, X. F. Le Goff, S. Maron, I. Maurin, F. Guillen, A. Garcia, T. Gacoin and J.-P. Boilot, *J. Am. Chem. Soc.*, 2010, **132**, 10967–10969.

3 Luminescent Pt(II)-complexes with metal···metal interactions:(*a*) M. Kato, *Bull. Chem. Soc. Jpn.*, 2007, **80**, 287–294; (*b*) V. N. Kozhevnikov, B. Donnio and D. W. Bruce, *Angew. Chem., Int. Ed.*, 2008, **47**, 6286–6289; (*c*) A. Aliprandi, D. Genovese, D. Mauro and L. De Cola, *Chem. Lett.*, 2015, **44**, 1152–1169; (*d*) K. Li, G. S. M. Tong, Q. Wan, C. G. Qingyun, W.-Y. Tong, W.-H. Ang, W.-L. Kwong and C.-M. Che, *Chem. Sci.*, 2016, **7**, 1653–1673; (*e*) A. Chowdhury, P. Howlader and P. S. Mukherjee, *Chem.–Eur. J.*, 2016, **22**, 1424–1434.

4 (*a*) X. Zhang, Z. Chi, Y. Zhang, S. Liu and J. Xu, *J. Mater. Chem. C*, 2013, **1**, 3376–3390; (*b*) P. Xue, J. Ding, P. Wang and R. Lu, *J. Mater. Chem. C*, 2016, **4**, 6688–6706.

5 Aqueous supramolecular hosts:(*a*) G. V. Oshovsky, D. N. Reinhoudt and W. Verboom, *Angew. Chem., Int. Ed.*, 2007, **46**, 2366–2393; (*b*) M. Yoshizawa, J. K. Klosterman and M. Fujita, *Angew. Chem., Int. Ed.*, 2009, **48**, 3418–3438; (*c*) T. R. Cook and P. J. Stang, *Chem. Rev.*, 2015, **115**, 7001–7045; (*d*) C. J. Brown, F. D. Toste, R. G. Bergman and K. N. Raymond, *Chem. Rev.*, 2015, **115**, 3012–3035; (*e*) J. Murray, K. Kim, T. Ogoshi, W. Yao and B. C. Gibb, *Chem. Soc. Rev.*, 2017, **46**, 2479–2496; (*f*) A. B. Grommet, M. Feller and R. Klajn, *Nat. Nanotechnol.*, 2020, **15**, 256–271; (*g*) Y. Yu, J.-M. Yang and J. Rebek Jr, *Chem*, 2020, **6**, 1265–1274; (*h*) E. G. Percástegui, T. K. Ronson and J. R. Nitschke, *Chem. Rev.*, 2020, **120**, 13480–13544; (*i*) L. Escobar and P. Ballester, *Chem. Rev.*, 2021, **121**, 2445–2514; (*j*) H. Takezawa and M. Fujita, *Bull. Chem. Soc. Jpn.*, 2021, **94**, 2351–2369; (*k*) D. Chakraborty and P. S. Mukherjee, *Chem. Commun.*, 2022, **58**, 5558–5573.

6 Y. Chen, K. Li, W. Lu, S. S.-Y. Chui, C.-W. Ma and C.-M. Che, *Angew. Chem., Int. Ed.*, 2009, **48**, 9909–9913.

7 (*a*) K. M.-C. Wong and V. W.-W. Yam, *Acc. Chem. Res.*, 2011, **44**, 424–434; (*b*) V. W.-W. Yam, V. K.-M. Au and S. Y.-L. Leung, *Chem. Rev.*, 2015, **115**, 7589–7728; (*c*) A. K.-W. Chan and V. W.-W. Yam, *Acc. Chem. Res.*, 2018, **51**, 3041–3051; (*d*) M. H.-Y. Chan and V. W.-W. Yam, *J. Am. Chem. Soc.*, 2022, **144**, 22805–22825.

8 (*a*) M. Mauro, A. Aliprandi, C. Cebrián, D. Wang, C. Kübel and L. De Cola, *Chem. Commun.*, 2014, **50**, 7269–7272; (*b*) A. Aliprandi, M. Mauro and L. De Cola, *Nat. Chem.*, 2016, **8**, 10–15.

9 Whereas the encapsulation of Pt(II)-complexes by coordination cages has been reported by several groups, the resultant host–guest systems show no luminescent properties:(*a*) M. Yoshizawa, K. Ono, K. Kumazawa, T. Kato and M. Fujita, *J. Am. Chem. Soc.*, 2005, **127**, 10800–10801; (*b*) J. E. M. Lewis, E. L. Gavey, S. A. Cameron and J. D. Crowley, *Chem. Sci.*, 2012, **3**, 778–784; (*c*) G. H. Clever, W. Kawamura, S. Tashiro and M. Shiro, *Angew. Chem., Int. Ed.*, 2012, **51**, 2606–2609.

10 We newly synthesized $(\mathbf{PBA})_n$ to compare the uptake and emission properties with those of $(\mathbf{PBS})_n$ reported previously (ref. 11).

11 Y. Okazawa, K. Kondo, M. Akita and M. Yoshizawa, *Chem. Sci.*, 2015, **6**, 5059–5062.

12 (*a*) K. Kondo, A. Suzuki, M. Akita and M. Yoshizawa, *Angew. Chem., Int. Ed.*, 2013, **52**, 2308–2312; (*b*) M. Kishimoto, K. Kondo, M. Akita and M. Yoshizawa, *Chem. Commun.*, 2017, **53**, 1425–1428; (*c*) Y. Satoh, L. Catti, M. Akita and M. Yoshizawa, *J. Am. Chem. Soc.*, 2019, **141**, 12268–12273.

13 Reviews on micellar aromatic capsules:(*a*) K. Kondo, J. K. Klosterman and M. Yoshizawa, *Chem.–Eur. J.*, 2017, **23**, 16710–16721; (*b*) M. Yoshizawa and L. Catti, *Acc. Chem. Res.*, 2019, **52**, 2392–2404; (*c*) M. Yoshizawa and L. Catti, *Proc. Jpn. Acad., Ser. B*, 2023, **99**, 29–38.

14 Y. Katagiri, Y. Tsuchida, Y. Matsuo and M. Yoshizawa, *J. Am. Chem. Soc.*, 2021, **143**, 21492–21496.

15 See the ESI†

16 The absorption band at $\lambda_{max} = 400$ nm can be assigned to the intramolecular metal-to-ligand charge transfer interactions of **1a** (ref. 6).

17 V. W.-W. Yam, K. H.-Y. Chan, K. M.-C. Wong and N. Zhu, *Chem.–Eur. J.*, 2005, **11**, 4535–4543.

18 The MCL properties of **1a–c** in solution as well as in the solid state have not been reported so far.[6] The observed high emissivity of $(\mathbf{PBA})_n \cdot (\mathbf{1a})_m$ even under aerobic conditions is most probably caused by full encircling of the hydrophobic $(\mathbf{1a})_m$ core by the hydrophobic bent frameworks of $(\mathbf{PBA})_n$ in water.

19 The manual grinding process as a mechanochemical stimulus is essential for (i) the formation of intermolecular metal···metal interactions of the Pt(II)-complexes and (ii) the enhancement of host–guest interactions to efficiently uptake the Pt(II)-complexes by the capsule in water. Although solids **1a–c** show solvation-dependent luminescence upon evaporation of their organic solutions (e.g., CH_2Cl_2, CH_3OH, acetone, and DMSO; Fig. S45†), the resultant solid-state emission properties cannot be maintained in solution.

20 (*a*) **BC** has been used as a dispersing luminogen in the OLEDs; (*b*) H. Uoyama, K. Goushi, K. Shizu, H. Nomura and C. Adachi, *Nature*, 2012, **492**, 234–238.

21 Vigorous stirring a mixture of **PBA**, **1a**, and **BC** in water gave rise to $(\mathbf{PBA})_n \cdot (\mathbf{1a})_m$ as a major product with low efficiency. The resultant host–guest composites showed weak green emission derived from monomeric **1a** (Fig. S42†).

22 The emission enhancement was observed upon irradiation at 450 nm, where there is no absorption band of **PBA** and **BC**, indicating the absence of host–guest and guest–guest energy transfer interactions.

23 H. Narita, L. Catti and M. Yoshizawa, *Angew. Chem., Int. Ed.*, 2021, **60**, 12791–12795.